Macromolecules
ARTICLE

Macromolecules **2010**, *43*, 1309–1318 **1309**
DOI: 10.1021/ma902356u

Stabilization of Amino Acid Derived Diblock Copolymer Micelles through Favorable D:L side chain interactions

Jared Skey,[†,‡] Claire F. Hansell,[†] and Rachel K. O'Reilly*[,†]

[†]*Department of Chemistry, University of Warwick, Coventry, CV4 7AL, U.K. and* [‡]*The Melville Laboratory for Polymer Synthesis, Department of Chemistry, University of Cambridge, Cambridge, CB2 1EW, U.K.*

Received October 22, 2009; Revised Manuscript Received December 11, 2009

ABSTRACT: Optically pure *N*-acryloyl-(D)-leucine methyl ester (D-Leu-OMe) (**1**) and *N*-acryloyl-(L)-leucine methyl ester (L-Leu-OMe) (**2**) were synthesized and studied using infrared spectroscopy and melting point analysis to determine if D–L interactions are preferential relative to D–D or L–L interactions. Reversible addition−fragmentation chain transfer (RAFT) polymerization yielded enantiopure homopolymers of D-Leu-OMe (**1**) and L-Leu-OMe ester (**2**). The two enantiopure polymers, **5** and **6**, and a 1:1 w/w racemic blend of both polymers were studied using infrared spectroscopy to investigate the intermolecular interactions in the polymeric systems. Poly(*tert*-butyl acrylate) [P(^{t}BuA)] macro chain transfer agents were used to synthesize two diblock copolymers from **1** and **2**, respectively. Subsequent deprotection of the P(^{t}BuA) block to poly(acrylic acid) (PAA) yielded two chiral amphiphilic diblock copolymers, **7** and **8**. Both enantiopure polymers were self-assembled separately and then in a 1:1 w/w ratio, and the resulting morphologies characterized using dynamic light scattering, atomic force microscopy, transmission electron microscopy, and circular dichroism.

1. Introduction

It has long been desirable to control the structure and properties of materials due to their widespread application in fields such as materials science and medicine.[1−8] New and existing methodologies have been developed and refined over the last 10 years, to aid the preparation and characterization of nanostructured materials. Of the many techniques that have been developed, one of the most widely employed for the synthesis of solution nanostructures with predictable properties is the self-assembly of block copolymers in mixed solvent systems.[9−19] Using this technique it is possible to produce different nanostructured materials with controlled and varied morphologies. Of these structures, core−shell type micelles are of interest as they bear a resemblance to constructs seen in biological systems. While being relatively stable in aqueous environments, these structures are held together through hydrophobic effects and hence are readily disrupted by ultrasound, heat or large changes in pH.[20−22] In some instances the instability of the particles under certain conditions is a useful property and has been exploited in many ways;[23−25] however, for other applications it is necessary for the particles to have much greater stability.

One way in which stability can be imparted is through cross-linking the core[26−29] or shell[30−33] of micelles to produce robust nanoparticles. Of these two approaches, one of the most widely used techniques is formation of covalent linkages in the hydrophilic corona of the particles. Although this technique facilitates the production of stable particles that are often biocompatible and capable of hydrophobic guest sequestration and transport—analogous to lipoproteins—the covalent cross-linking of the particles may lead to a reduction in encapsulation efficiency, hydrophilicity, or biodegradability. As an alternative to chemically cross-linking the shell, stability can come from dynamic polymer−polymer interactions with examples including polyelectrolyte,[34−37] stereocomplex,[38] and hydrogen bonding[39] complex formation in the core between the hydrophobic blocks or in the shell between the hydrophilic blocks.

Stereocomplex formation between polymers has been known since 1968 when Liu and Liu published their results on stereoregular poly(methyl methacrylate).[40] They saw that stereocomplexation occurred between isotactic poly(methyl methacrylate) (iPMMA) and syndiotactic poly(methyl methacrylate) (sPMMA). Further work done on the system using X-ray fiber diffraction showed that the stereocomplex exists in a two-state rotationally disordered double-stranded helix, having an asymmetric unit consisting of one iPMMA unit and two sPMMA units.[41] The mechanical and physical properties of the stereocomplexed PMMA were investigated and a synergistic effect was observed.[42,43] Since it has been known that stereocomplexation between polymers is possible many groups have investigated the interactions exhibited between stereoregular chains of polylactides and poly(lactic acids).[44−47] Both of these polymers can be synthesized from optically pure monomer sources with retention of chirality at the carbon stereocenter to yield stereoregular polymers. The initial work carried out in the area of stereocomplexation between polymeric D- and L-lactides was first reported in 1987 by Ikada and Tsuji.[48] They were able to show that polymers synthesized from racemic lactide were amorphous, those synthesized from optically pure D- or L-lactide yielded crystalline polymers and furthermore, an equimolar blend of poly(D-lactide) and poly(L-lactide) also gave crystalline polymers. Using differential scanning calorimetry (DSC) they were able to show a positive shift in the melting temperature of 50 °C, which was indicative of the formation of a stereocomplex between the two enantiopure polymers. Since 1987, a considerable amount of work has been undertaken to understand how different factors contribute to the formation of the homo- and heterocrystalline polymers. The factors found to promote stereocomplex formation are the molar ratio of D:L lactide units in the blend (with equimolar amounts giving the best results) and a compromise between a low molecular weight and a sufficiently long enough chain length in both of the isomeric polymers.[49]

*Corresponding author.

Published on Web 01/07/2010

While the stereocomplex formation between the two enantiomers of polylactide has been widely studied, applications deriving from this interaction have not yet been so widely investigated. Leroux et al. first described how amphiphilic diblocks containing poly(ethylene glycol) (PEG) as the hydrophilic block and either poly(D-lactide) or poly(L-lactide) as the hydrophobic block could be self-assembled to make micellar type structures.[50] The micelles made from an equimolar blend of D-lactide containing and L-lactide containing amphiphiles had kinetic stability and redispersion properties superior to micelles prepared with isotactic or racemic polymers alone. The same stereocomplex interaction was utilized by Hedrick et al. to stabilize mixed micelles where the hydrophilic segment of the diblock was either PEG or *N*-isopropylacrylamide.[51] Without the stabilization imparted by the stereocomplex it was proposed that the structures would have fallen apart or would have formed two populations of nonmixed micelles due to the incompatibility of the two hydrophilic species.

Work done by Lecommandoux et al. has focused largely upon micelles and vesicles or "polymersomes" made of diblock copolymers where at least one of the blocks is a main chain polypeptide. Exploiting the formation of α-helices as a response to a change in pH has been shown to be a suitable driving force for self-assembly.[52] The formation of secondary structures in the micelle cores and vesicle membranes has been observed to impart greater stability to the nanostructures. More recently, interesting work has been undertaken by Adams and Young et al. to demonstrate the inclusion of oligopeptides up to trimers into the side chains of methacrylate polymers and the subsequent self-assembly of these systems into vesicles.[53] Using circular dichroism they were able to show the formation of secondary structures between the hydrophobic methacrylate chains bearing pendant oligopeptide units. These structures were thought to form in both an inter- and an intramolecular fashion. When these systems were investigated using diblocks made from complementary isomers no beneficial behavior was exhibited, however it was observed that interactions between polymers containing amino acid residues could be used to stabilize self-assembled nanostructures.

Of great interest due to the abundance of enantiomerically pure natural and non-natural amino acids, is the potential formation of a stereocomplex that could arise between vinyl polymers containing pendant amino acid derivatives. In nature, different amino acids are joined together through a series of amide bonds to form polypeptides. In an attempt to understand the roles that the different amino acids can play in polymer structure and function, the incorporation of amino acids into synthetic polymers has, understandably, been of interest for some time. The group headed by Endo has been instrumental in the synthesis and characterization of polymers from vinyl derivatives of amino acids.[54−57] Using reversible addition−fragmentation chain transfer (RAFT) techniques, they have shown that it is possible to synthesize polymers with controlled molecular weights and narrow dispersities, containing pendant amino acids.[58,59] Indeed, in 1996, Endo et al. reported their findings on the formation of a racemic stereocomplex between methacrylamide monomers derived from L- and D-leucine methyl ester.[60] Other work, carried out in the group of McCormick, has investigated the relationship between optical activity and the ratio of *N*-acryloyl-L-alanine relative to *N*-acryloyl-D-alanine in the polymer composition. Relative to enantiomorphic small molecules, it was seen that incorporating the amino acids within a polymer chain had a synergistic effect on the optical activity of the samples.[61]

What has become apparent in naturally occurring systems is that the formation of recognizable structural motifs arises from the inherent chirality of amino acids and the hydrogen bonding interactions between the different moieties. Specific assembly or recognition events between synthetic polymers can be targeted through direct incorporation of amino acid based monomers and exploiting the interactions seen in natural systems. Formation of α-helices in synthetic oligopeptide and polypeptide chains is seen to be energetically favorable when the peptide is made entirely from optically pure L-leucine.[62,63] Using vinyl derivatives of L-leucine, different groups have tried to replicate this self-assembly but the results are somewhat ambiguous.[64,65]

By synthesizing amphiphilic diblocks where one block contains an enantiomerically pure amino acid derivative it may prove possible to synthesize stereocomplex stabilized micelles with mixed core and/or mixed shell domains. This could potentially remove the need to chemically cross-link particles and instead stabilize them through stereocomplex formation. Until now a side-chain stereocomplex interaction between isomeric polymers has not been reported to the best of our knowledge. The results herein discuss the interactions between the monomeric and polymeric forms of enantiopure D- and L-*N*-acryloyl leucine methyl ester and the resulting effects that these interactions have on the nanostructures formed from the respective amphiphilic diblock copolymers. Amplifying these interactions to increase the stability of particles made from these polymers could be of interest in the field of drug delivery where it is important for the body to be able excrete any vectors used to get the drug into the body. Currently these vectors can take the shape of core/shell type structures that are often stabilized with covalent linkages. While work that has been carried out to increase stability without the need for covalent linkages has been successful (such as the stereocomplexation between isomeric stereoregular polylactides), the versatility of the systems is limited by availability of monomers. Using both natural and synthetic amino acid derived vinyl monomers opens up a vast toolbox of optically pure, functionalized monomers that can potentially be used to tailor the properties (such as strength of interaction, processability, drug affinity) of individual micelle populations. It is further envisaged that populations of mixed micelles resulting from polymer chains incorporating different amino acids with opposing chirality could enable fine-tuning of these systems.

2. Experimental Section

Materials. (2,2′-Azobis(2-methylpropionitrile) (AIBN, 98% from Sigma-Aldrich) was recrystallized twice from methanol and stored in the dark at 4 °C. ^{t}BuA (98%) was distilled over CaH_2 and stored at 4 °C. D-Leu-OMe, (**1**), and L-Leu-OMe, (**2**), were synthesized using a literature preparation.[66] Benzyl biphenyl-4-carbodithioate, (**3**), and Poly(*tert*-butyl acrylate) [P(^{t}BuA)] macroCTA (**4**) (M_n = 1.2 × 10^3 g mol^{-1}, M_w/M_n = 1.10) were synthesized as previously reported.[67] All other reagents were purchased from Sigma-Aldrich and were used without further purification.

Instrumentation. ^{1}H and ^{13}C spectra were recorded at 300 or 400 MHz and ^{13}C at 75 MHz with Bruker DPX-300/DPX-400 spectrometer using $CDCl_3$ or DMSO-d_6. Chemical shifts are reported in ppm (δ) relative to $CHCl_3$ (7.26 ppm for ^{1}H and 77.2 ppm for ^{13}C) or DMSO-d_6 (2.50 ppm for ^{1}H) as internal reference. Gel Permeation Chromatography (GPC) data for all polymers were obtained on a Spark Basic+ Marathon autosampler with a LC1120 HPLC pump (Polymer Laboratories) with and a DRI detector from polymer laboratories. Two PLgel 5 μm mixed C columns with a PLgel 5 μm Guard column were used at 40 °C with a dimethylformamide (DMF) flow rate 0.8 mL min^{-1}. All molecular weights are relative to PMMA standards. IR spectra were obtained on Perkin-Elmer Spectrum 100 ATR FT-IR spectrometer. Hydrodynamic diameters (D_h) and size distributions for the micelles in aqueous solutions were determined by dynamic light scattering (DLS). The DLS measurements were taken on a Malvern Nano S Zetasizer Nano Series instrument. Prior to analysis, solutions were filtered

through a 0.45 μm nylon syringe filter to remove any dust or particulate matter. The height measurements and distributions for the nanoparticles were determined by tapping-mode Atomic Force Microscopy (AFM) under ambient conditions in air. The AFM instrumentation consisted of a Veeco Multimode V system equipped with Nanoscope V Controller (Digital Instruments, Veeco Metrology Group; Santa Barbara, CA) and standard silicon RFESP type tips (spring constant, 3 N/m; *L*, 225 μm; resonant frequency, 75 kHz). The samples were prepared for AFM analysis by drop deposition of approximately 0.1 mL of sample at a concentration of approximately 0.2 g dm^{-3} onto freshly cleaved mica and allowed to dry freely in air. The number-average particle heights (H_{av}) and diameter (D_{av}) values and standard deviations were generated from the sectional analysis of 100 particles from five different analysis regions. Transmission electron microscopy samples were prepared by drop deposition onto copper/carbon grids that had been treated with oxygen plasma to increase the surface hydrophilicity. The particles were stained using a dilute 5% aqueous solution of uranyl acetate. Micrographs were collected at magnifications varying from 25 K - 60 K and calibrated digitally. Number-average particle diameters (D_{av}) and standard deviations were generated from the analysis of a minimum of 150 particles from at least three different micrographs. Specific rotation data was collected on an Optical Activity AA-10 automatic polarimeter with a mercury lamp (546 nm). All melting points were measured on a Gallenkamp melting point apparatus. CD spectra were collected on a Jasco J-715 spectropolarimeter with a water baseline subtracted from each data set.

Methods. *Synthesis of Poly(tert-butyl acrylate) [P(ᵗBuA)] macroCTA* (***4***). **4** was prepared as follows: *tert*-butyl acrylate (3.0 g, 23.6 mmol), CTA **2** (0.038 g, 0.118 mmol), and AIBN (0.0019 g, 0.0118 mmol) were placed in a dry glass ampule equipped with magnetic stirrer bar and the solution was degassed by 3× freeze−evacuate−thaw cycles. The sealed vessel was then held at 80 °C for 3 h. After polymerization had occurred the ampules were cooled in liquid N_2 and the reaction mixture was diluted with THF. The polymer was precipitated twice into a stirred solution of cold methanol/water (10:2 v/v), allowed to stand and then the solvent was decanted off. After being dried over magnesium sulfate, the polymer was dried overnight at room temperature under vacuum and isolated as a pale pink glassy solid. Conversions were calculated using ^{1}H NMR spectroscopy by comparing the vinyl signals of the monomer (δ ca. 5.65) with the backbone signals of the polymer and the *tert*-butyl groups of both monomer and polymer (δ ca.1.10−2.35). ^{1}H NMR (500 MHz, $CDCl_3$): δ_H = 8.1−6.9 (Ar−*H* from initiator, m), 2.5−2.1 (C*H* of the polymer backbone, br), 1.9−1.7 (CH_2 of the polymer backbone, br), 1.7−1.0 (C(CH_3)$_3$ group, br). ν_{max} (cm^{-1}) = 2974, 2928, 1723, 1391, 1366, 1252, 1142, 844. M_n^{NMR}($CDCl_3$) = 11.5 kDa; M_n^{GPC}($CHCl_3$) = 12.1 kDa; M_w/M_n = 1.10.

Synthesis of Poly(D-Leu-OMe) (***5***) *and Poly(L-Leu-OMe)* (***6***). An example is as follows: D-Leu-OMe (**1**) (0.5 g, 2.512 mmol), **3** (0.004 g, 0.0125 mmol), AIBN (0.0002 g, 0.0013 mmol), and dioxane ([M] = 0.718 mol dm^{-3}) were placed in a dry glass ampule equipped with magnetic stirrer bar. The solution was degassed by 3× freeze−pump−thaw cycles. The vessel was sealed and stirred at 90 °C for the required amount of time. After polymerization had occurred the ampules were cooled in liquid N_2 and further dioxane (5 mL) was added from which the polymers were isolated after freeze-drying. Conversions were calculated using ^{1}H NMR spectroscopy by removing an aliquot prior to precipitation and comparing the vinyl signals of the monomer (δ = 5.59) with the chiral proton of both monomer and polymer (δ = 4.11−4.82). ^{1}H NMR ($CDCl_3$) δ = 4.30−4.85 (br, CH_2C**H**), 3.57−3.92 (br, CO_2CH_3), 1.15−2.52 (br, CH_2-^{i}Pr; br C**H** backbone; br, CH_2, backbone), 0.72−1.14 (br, C**H**−(CH_3)$_2$). ν (cm^{-1}) = 3331, 2959, 1728, 1656, 1539, 1441, 1370, 1208, 1157, 984.

5, P(D-Leu-OMe): M_n^{GPC}(DMF) = 2.2×10^4 g mol^{-1}, M_w/M_n = 1.20.

6, P(L-Leu-OMe): M_n^{GPC}(DMF) = 1.5×10^4 g mol^{-1}, M_w/M_n = 1.28.

Chain Extension of ***4*** *with* ***1*** *or* ***2*** *To Afford P(ᵗBuA)-b-P(D-Leu-OMe)* (***7***) *and P(ᵗBuA)-b-P(L-Leu-OMe)* (***8***), *Respectively*. An example is as follows: MacroCTA (**4**) (0.318 g, 0.0262 mmol), (**2**) (0.523 g, 2.63 mmol), AIBN (0.0004 g, 0.0026 mmol) and dioxane ([M] = 0.718 mol dm^{-3}) were placed in a dry glass ampule equipped with magnetic stirrer bar. The solution was degassed using 3× freeze−pump−thaw cycles. The vessel was then sealed and held at 90 °C for 14 h. After this time the ampules were cooled in liquid N_2 and the reaction mixture diluted with THF as necessary. The polymers were precipitated into a stirred cold solution of MeOH: water (1:1), allowed to stand and then the solvent was decanted off. After addition of dioxane the polymers were dried over magnesium sulfate and then freeze-dried to yield a pale pink or off white powder. ^{1}H NMR ($CDCl_3$) δ = 4.30−4.85 (br, CH_2C**H**), 3.57−3.92 (br, CO_2CH_3), 1.15−2.52 (br, CH_2-^{i}Pr; br, C**H** backbone; br, CH_2 backbone, C(CH_3)$_3$), 0.72−1.14 (br, C**H**-(CH_3)$_2$). ν (cm^{-1}) = 2960, 2920, 1725, 1656, 1533, 1440, 1208, 1146, 845.

P(ᵗBuA)-*b*-P(*D*-Leu-OMe) (**7**): M_n^{NMR} ($CHCl_3$) = 3.1×10^4 g mol^{-1}; M_n^{GPC} (DMF) = 16.4×10^3; M_w/M_n = 1.32.

P(ᵗBuA)-*b*-P(*L*-Leu-OMe) (**8**): M_n^{NMR} ($CHCl_3$) = 25.8×10^3 g mol^{-1}; M_n^{GPC} (DMF) = 14.2×10^4; M_w/M_n = 1.26.

Deprotection of ***7*** *and* ***8*** *To Give PAA-b-P(D-Leu-OMe)* (***9***) *and PAA-b-P(D-Leu-OMe)* (***10***), *Respectively*. An example is as follows: Polymer **8** (0.60 g, 0.0191 mmol) was dissolved in dichloromethane (20 mL) and cooled to 0 °C. Trifluoroacetic acid (2.42 g, 16.81 mmol, 10 equiv with respect to ᵗBuA units) was added dropwise and the solution was stirred at room temperature for 19 h. The solvent and excess acid were driven off under a flow of air. The resulting brown gum was dissolved in THF:water (1:1), dialyzed (MWCO point of tubing = 3.5 kDa) into pure water over 30 h (5× water changes) and then lyophilized to yield a pale pink or off white powder. ^{1}H NMR (DMSO-d_6, ppm): δ = 11.91−12.82 (br, COO**H**), 7.3−8.4 (br, N−**H**), 4.30−4.85 (br, CH_2C**H**), 3.57−3.92 (br, CO_2CH_3), 1.15−2.52 (br, CH_2-^{i}Pr; br, C**H** backbone; br, CH_2 backbone), 0.72−1.14 (br, C**H**-(CH_3)$_2$). ν (cm^{-1}) = 3600−2500 (broad carboxylic acid signal), 2956, 1728, 1659 (broad signal), 1536, 1441, 1209, 1161, 802.

PAA-*b*-P(*D*-Leu-OMe) (**9**): M_n^{NMR} (DMSO-d_6) = 2.6×10^4 g mol^{-1}.

PAA-*b*-P(*L*-Leu-OMe) (**10**): M_n^{NMR} (DMSO-d_6) = 2.1×10^4 g mol^{-1}.

Micellization of ***9***, ***10***, *and a 1:1 Molar Ratio of* ***9*** *and* ***10*** *To Afford* ***11***, ***12***, *and* ***13***, *Respectively*. An example is as follows: A round-bottom flask equipped with a stirrer bar was charged with (**9**) (0.1 g), DMF (100 mL) was added and the solution was allowed to stir at room temperature for 30 min to ensure that the mixture was homogeneous. Nanopure water (100 mL) was added to the rapidly agitated solution via a peristaltic pump at the rate of 15 mL h^{-1}. After all of the water had been added, the bluish micelle solution was transferred to dialysis tubing (MWCO *ca.* 12−14 kg mol^{-1}), and dialyzed against nanopure water for 7 days with regular water changes, to remove all of the residual DMF.

11. The final polymer concentration was 0.34 g dm^{-3}. D_h (DLS) = 32 nm (PDI = 0.20); D_{av} (TEM) = 21 ± 4 nm. Lyophilization gave **11** as a white solid.

12. The final polymer concentration was 0.27 g dm^{-3}. D_h (DLS) = 27 nm (PDI = 0.15); D_{av} (TEM) = 18 ± 5 nm. Lyophilization gave **12** as a white solid.

13. The final polymer concentration was 0.31 g dm^{-3}. D_h (DLS) = 51 nm (PDI = 0.44); D_{av} (TEM) = 31 ± 6 nm. Lyophilization gave **13** as a white solid.

3. Results and Discussion

Monomer Synthesis. The D (**1**) and L (**2**) enantiomers of the monomer *N*-acryloyl leucine methyl ester were synthesized

Table 1. Melting Point and IR Spectroscopy Data for Samples with Varying Compositions of 1 and 2 (br = Broad Signal)

				ν_{N-H} stretch (cm^{-1})		ν_{N-H} bend (cm^{-1})		
	D:L ratio	$[\alpha]_{546}^{25}$(deg)	melting point (°C)					$\nu_{C=O}$ ester stretch (cm^{-1})
i	100:0	+72	55−57	3284		1626	1619	1749
ii	80:20	a	62−63	3281	3251	1627	1620	1746
iii	60:40	a	76−78		3249 (br)	1627		1746
iv	50:50	0	79−81		3242	1628		1743
v	40:60	a	76−78		3247 (br)	1627		1744
vi	20:80	a	62−63	3283	3249	1627	1619	1745
vii	0:100	−73	55−57	3287		1627	1619	1749

[a] Not measured.

from a modified literature preparation by reacting the respective D and L enantiomers of the hydrochloride salt of leucine methyl ester with acryloyl chloride in yields of 82 and 77% respectively.[66] The structure and properties of both monomers were successfully characterized using ^{1}H and ^{13}C NMR, infrared spectroscopy and melting point analysis.

*Investigation into Stereocomplex Formation between D-Leu-OMe (**1**) and L-Leu-OMe (**2**).* Previous work undertaken by Endo et al. on the methacryloyl derivatives of the monomers being studied in this report, indicated, through the use of melting points and X-ray crystallographic data, that stereocomplexes between these moieties do exist.[60] They showed the existence of an intermolecular hydrogen bond between the amide proton on one enantiomer and the corresponding amide carbonyl on the opposite enantiomer. The stereocomplex formation between the D and L enantiomers of the monomers being used in this study was investigated using melting point analysis and infrared spectroscopy. Seven solutions, i−vii, containing different compositions of D and L monomer were made up in chloroform and the solvent was allowed to evaporate overnight. Simple melting point determination of the resulting solids showed that as the samples go from optically pure toward a racemate, the melting point increases steadily (Table 1). It can also be seen that regardless of which monomer is present in greater amounts, if the ratios are the same then the melting point of the solid is identical, which would be expected as there is no physical difference between the two enantiomers. This result indicates that the two enantiomers may be forming a racemic stereocomplex that exhibits a synergistic stability toward temperature. Furthermore, when comparing the specific rotation values for the enantiopure monomers as expected it can be seen that the numbers only differ within experimental error and sign.

Stereocomplex formation was further evidenced by differences in the infrared spectra of samples i−vii (Table 1). Of initial interest is the marked difference in the stretching frequency of the amide proton. In both enantiomerically pure samples (entries i and vii in Table 1) the peak is relatively sharp and appears at approximately 3285 cm^{-1}. The amide proton environment that this signal relates to can be considered a "free" or "non hydrogen bonded" environment. As the sample becomes increasingly racemic the appearance of a second peak at ~3250 cm^{-1} is noticed. This can be attributed to the formation of two three-centered intermolecular hydrogen bonds between the two enantiomers similar to that seen in the work by Endo.[60] When the composition of the sample is equimolar (entry iv in Table 1) the band at ~3285 cm^{-1} has disappeared completely which suggests the formation of the racemic stereocomplex is quantitative. This red-shift has been observed in other hydrogen bonding interactions and is well documented in the literature.[68] This would suggest that the heterointeraction (D–L) is highly favorable compared with the homointeractions (D-D or L–L). Also indicative of the formation of the racemic stereocomplex is the shift in bending frequency of the amide proton. In the enantiomerically pure samples the bending is anisotropic leading to two well-defined signals at 1619 and 1627 cm^{-1} (see Supporting Information). The presence of two signals is often observed with amides, however in the equimolar mixture only one signal is seen, although it is slightly broader than in the enantiomerically pure samples. It is postulated that once the stereocomplex has formed it reduces the freedom of the N−H bond to vibrate. There is also a 6 cm^{-1} red shift in position of the ester carbonyl from 1749 to 1743 cm^{-1} when moving from the enantiomerically pure system to the racemate. Interestingly there is no shift in the amide carbonyl absorbance which appears consistently at 1656 cm^{-1}. This may point toward the hydrogen bonding interaction involving the ester carbonyl rather than the amide carbonyl as seen in the methacryloyl derivatives.

*Synthesis of Enantiomerically Pure Homopolymers from D-Leu-OMe (**1**) and L-Leu-OMe (**2**).* Both enantiomeric forms of the monomer were polymerized to afford two samples of enantiomerically pure homopolymer (**5** and **6**). A chain transfer agent (CTA) and reaction conditions identical with those reported in previous work[67] using *N*-acryloyl-L-phenylalanine were used to synthesize the polymers (Scheme 1). Both polymerizations went to high conversion and proceeded in a controlled manner with reasonable control over the molecular weight and dispersity. The conversion was calculated by ^{1}H NMR spectroscopy by comparing the signal at $\delta = 5.71$ (which equates to 1 proton in the monomer) with the signal at $\delta = 4.19-4.66$ (which equates to 1 proton in the polymer). The molecular weight determined from analysis by DMF GPC (which had been calibrated to PMMA narrow standards) was somewhat distorted due to the dissimilar nature of the polymers compared with PMMA. To overcome this problem ^{1}H NMR spectroscopy would normally be used to calculate the molecular weights via end group analysis however this was not possible due to the amide proton obscuring the region where the end group signal resonances occur. Ultimately, for the purposes of this study, control of the block length and molecular weight were unnecessary. The characterization data is summarized in Table 2.

The data shown in Figure 1 indicate that the polymerization of *N*-acryloyl-L-leucine methyl ester proceeds in a controlled manner as it exhibits linear kinetics when comparing monomer conversion with time. An induction period of approximately 55 min is observed; the reasons for induction periods in RAFT polymerizations are discussed elsewhere in the literature, it suffices to say that they cannot be predicted and depend upon CTA choice, the monomer and the polymerization conditions.[69,70] As there is no chemical difference between the D and L forms of the monomer the kinetic data can be assumed to be identical for both systems.

*Investigation into Stereocomplex Formation between **5** and **6**.* As discussed previously the formation of a racemic stereocomplex between the two enantiomers of the monomer

Scheme 1. AIBN-Initiated, Solution RAFT Polymerization of *N*-Acryloyl-(D)-leucine Methyl Ester (1) and *N*-Acryloyl-(L)-leucine Methyl Ester (2) Using Benzyl Biphenyl-4-carbodithioate (3) at 90 °C in Dioxane where [M] = 0.743 mol dm^{-3} and M:3:AIBN = 200:1:0.1

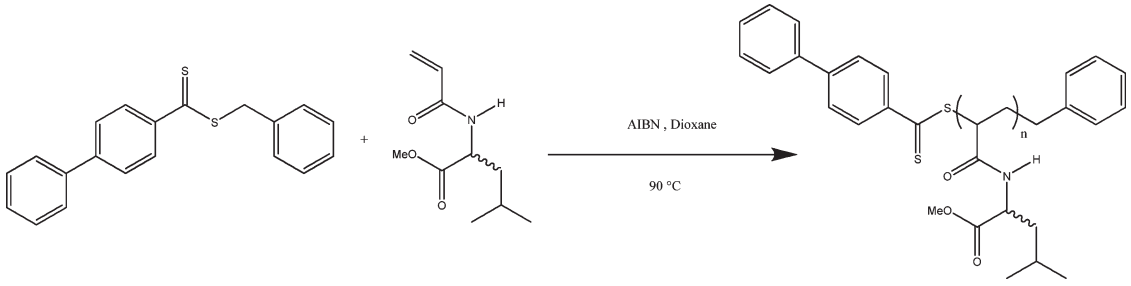

(3)

(1) = *D*-Leu-OMe
(2) = *L*-Leu-OMe

(5) = P(*D*-Leu-OMe)
(6) = P(*L*-Leu-OMe)

Table 2. Polymerization Conditions and characterization data for all homopolymers synthesized using either *N*-acryloyl-(D)-leucine methyl ester, (1), or *N*-acryloyl-(L)-leucine methyl ester, (2), and benzyl biphenyl-4-carbodithioate, (3). For all polymerizations M:(3):AIBN = 200:1:0.1. Solution polymerizations carried out in dioxane

monomer	[M] (mol dm^{-3})	time (min)	convn (%)	$M_{n,th}$ (kDa)	M_n^{NMR} (kDa)	M_n^{GPC} (kDa)	M_w/M_n
D	0.743	1380	85	33.8	a	22.0[b]	1.20
L	0.743	1350	86	34.3	a	15.0[b]	1.28
tert-butyl acrylate	bulk	180	49	12.8	11.5	12.1[c]	1.10

[a] amide proton obscured the region where the end group signal resonances occur preventing molecular weight determination by end group analysis. [b] DMF GPC data is relative to a PMMA calibration. [c] $CHCl_3$ GPC data is relative to a PMMA calibration.

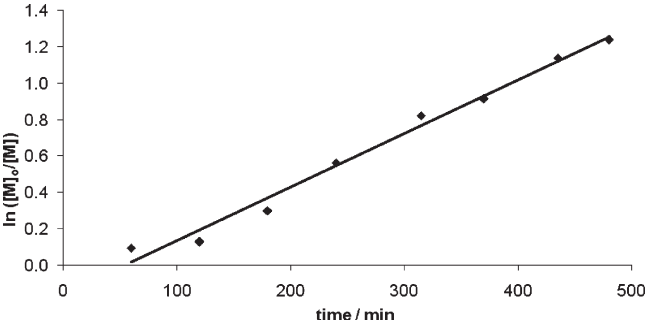

Figure 1. Kinetic plot for the polymerization of of *N*-acryloyl-(L)-leucine methyl ester (**2**) in dioxane using benzyl biphenyl-4-carbodithioate (**3**). Polymerization carried out at 90 °C in dioxane where [M] = 0.743 mol dm^{-3} and **2**:**3**:AIBN = 200:1:0.1. k_p = 0.0029 min^{-1}.

can be easily characterized by the red shift of the N−H stretching frequency and the resolution into one peak of the N−H bending frequency in the infrared spectrum. To investigate whether this phenomenon occurred in the polymeric system the spectra of both homopolymers and a 1:1 w/w blend of both homopolymers were recorded. The blend was prepared by dissolving 50 mg of both blocks in dioxane and subsequently removing the solvent by freeze-drying.

The first observation to be noted is that the N−H stretching frequency in the enantiomerically pure homopolymers has a blue shift of approximately 50 cm^{-1} compared with the values seen for the corresponding monomers (Table 3). This may indicate that in the monomer there is some form of intermolecular hydrogen bonding interaction occurring similar to, but weaker than, that proposed for the racemic stereocomplex. Once the monomer is incorporated into a polymer chain it may not be as easy for the pendant leucine groups to get into the right orientation for this interaction to occur. In the racemic blend of both homopolymers the predominant N−H stretching frequency is almost identical to that seen in the stereocomplexed monomers, which is evidence for the formation of a stereocomplex between the two homopolymer chains. Also apparent in the infrared spectrum is the difference in the N−H bending frequency when comparing the enantiopure monomers to their respective polymers. The peak has a blue shift of about 30 cm^{-1} which is again indicative of a difference in the conformation of the hydrogen bonding environment. There is also a significant amount of broadening in this signal in the polymers and only one signal is observed. In the racemic polymeric systems, the appearance of a second peak and the sharpness of this and the nonshifted peak relative to the monomer are the most striking observations. Further evidence for the racemic stereocomplex is the red shift of about 20 cm^{-1} and change in shape of the ester carbonyl stretching frequency in the enantiomerically pure samples. In the racemic blend, this signal does not move and retains its sharpness (Figure 2).

In general, the spectrum of the racemic blend is much sharper and well-defined however many of the signals have slight shoulders appearing at the frequencies seen in the enantiopure homopolymers which are not seen in the racemate of the monomers. When considering that the racemic stereocomplex is definitely the preferred conformation in a racemate of the monomers due to the increased stability, the same could be expected in the racemic polymer blend. It would be fair to say that although the interaction is still present it is not possible for all of the polymer chains to orient themselves in such a way so that every monomer unit in the chain is able to form a racemic stereocomplex. This could be due to the entanglement between the chains and goes some way toward explaining why there is a presence of signals from nonstereocomplexed units in the polymer chain whereas in the racemic monomer there is >99% stereocomplexation occurring. The exact nature of the stereocomplex formed through a heterointeraction between D and L blocks is not known but from the IR data it appears to be the predominant and most stable orientation compared with the homointeraction between either D and D or L and L homopolymers (Figure 2).

Synthesis of ^{t}BuA MacroCTA. The *pseudo*-living free radical polymerization of ^{t}BuA using **3** has been reported previously.[67] Using this literature preparation it was possible to synthesize a ^{t}BuA homopolymer with a predicted M_n and

Table 3. Infrared Spectroscopy Data for Poly(*N*-acryloyl-(D)-leucine methyl ester) (5) and Poly(*N*-acryloyl-(L)-leucine methyl ester) (6)[a]

		ν_{N-H} stretch (cm^{-1})			ν_{N-H} bend (cm^{-1})			$\nu_{C=O}$ ester stretch (cm^{-1})
	D:L ratio							
i′	100:0	3331			1656 (br)			1728 (br)
vii′	0:100	3331			1656 (br)			1729 (br)
iv′	50:50	3332[b]		3245	1655	1629		1744
i	100:0		3284			1626	1619	1749
iv	50:50			3242		1628		1743

[a] Entries i and iv are reproduced from Table 1 for comparison. Broad signals are denoted by (br). [b] Peak only just visible.

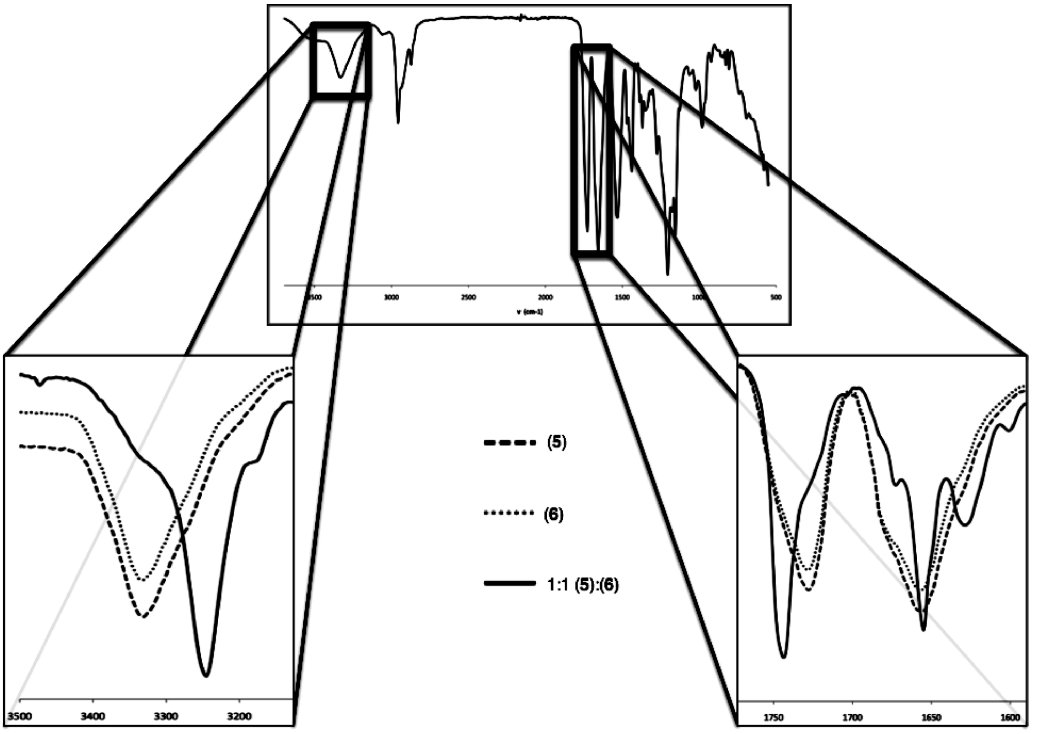

Figure 2. IR spectra of poly(*N*-acryloyl-D-leucine methyl ester) (**5**). Insets show certain areas of interest for **5**, poly(*N*-acryloyl-L-leucine methyl ester) (**6**), and a racemic blend of **5** and **6** in greater detail.

Scheme 2. Depiction of the AIBN-Initiated, Bulk RAFT Polymerization of *tert*-Butyl Acrylate Using Benzyl Biphenyl-4-carbodithioate (3) at 80 °C where M:3:AIBN = 200:1:0.1

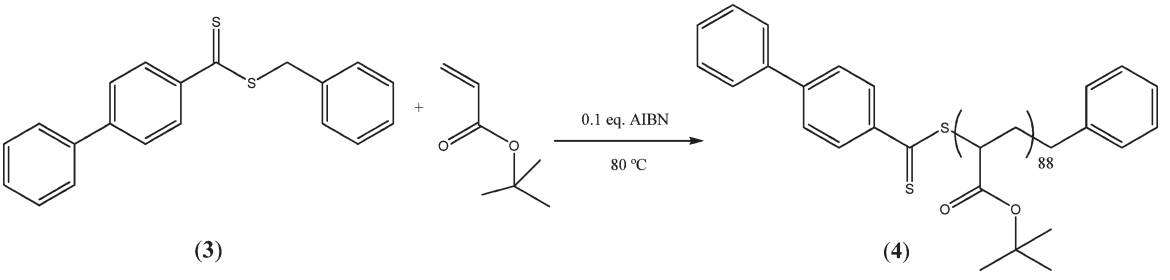

narrow dispersity (Scheme 2). The polymerization was allowed to run for 3 h after which time it was quenched in liquid N_2 and was found to have gone to 49% conversion by ^{1}H NMR spectroscopy. This was calculated by comparing the vinyl signals of the monomer with the backbone and *tert*-butyl signals of the monomer and polymer. The molecular weight of the polymer was determined using ^{1}H NMR spectroscopy with extended scans (11.5 kDa) and GPC analysis in DMF calibrated to PMMA (12.1 kDa) with a dispersity (M_w/M_n) of 1.10.

Chain Extension of MacroCTA (4) with D-Leu-OMe (1) or L-Leu-OMe (2). The chain extension of **4** with D-Leu-OMe, (**1**) (Scheme 3), was carried out over 16 h at 90 °C in dioxane with a M:**4**:AIBN ratio of 100:1:0.1. After analysis of the resulting solution by ^{1}H NMR spectroscopy the polymerization was found to have gone to 89% conversion. The molecular weight (31.4 kDa) of the isolated diblock was calculated by comparing the signal at δ = 4.19 - 4.66 (1 acrylamide proton) with the signal at δ = 0.61 - 2.55 (8 protons from the backbone and isopropyl group of the acrylamide and 12 protons from the backbone and *tert*-butyl group of the ^{t}BuA). The dispersity (M_w/M_n = 1.37) of the diblock copolymer was further characterized using GPC analysis in DMF again calibrated with PMMA. The trace obtained from the DMF GPC indicated that the polymerization proceeded in a controlled manner as the signal was

Scheme 3. Chain Extension of Poly(*tert*-butyl acrylate) (4) with *N*-Acryloyl-(D)-leucine Methyl Ester (1) or *N*-Acryloyl-(L)-leucine Methyl Ester (2) in Dioxane ([M] = 0.718 mol dm^{-3}) at 90 °C. M:4:AIBN = 100:1:0.1

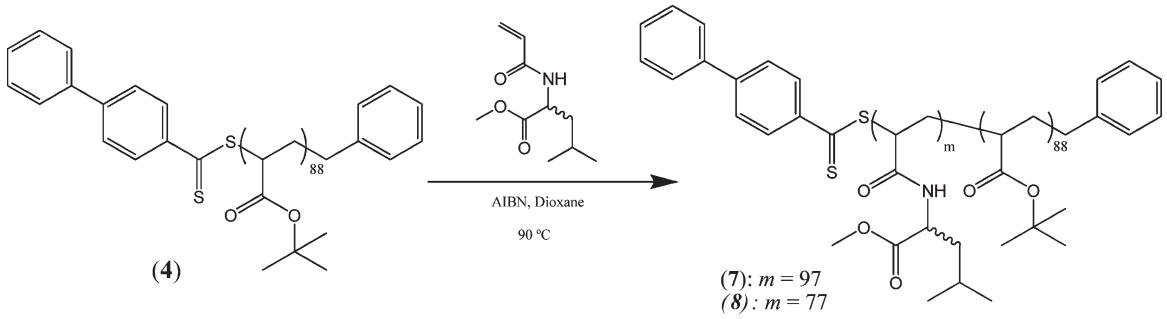

Table 4. Polymerization Data for Chain Extension of Poly(*tert*-butyl acrylate)$_{88}$, (4), with *N*-Acryloyl-D-leucine Methyl Ester (1) and *N*-Acryloyl-L-leucine Methyl Ester (2) in dioxane ([M] = 0.718 mol dm^{-3}) at 90 °C carried out over 960 min, M:4:AIBN = 100:1:0.1

polymer	*m*	convn (%)	M_n^{NMR} (kDa)	M_n^{GPC} (kDa)	$M_{n,th}$ (kDa)	M_w/M_n
7	97	89	31.4	16.4	29.2	1.37
8	77	71	25.8	14.2	25.3	1.26

unimodal which suggests that all of the macroCTA was chain extended. An identical procedure was undertaken with the second chiral monomer (**2**), and similar results were obtained (Table 4). In both cases the chain extension was shown to proceed well as the GPC traces showed monodisperse populations of polymer with reasonably narrow molecular weight distributions (see ESI).

*Deprotection of P(D-Leu-OMe)-b-P(^{t}BuA) (**7**) and P(L-Leu-OMe)-b-P(^{t}BuA) (**8**) To Form Amphiphilic P(D-Leu-OMe)-b-P(AA) (**9**) and P(L-Leu-OMe)-b-P(AA) (**10**).* In both the D- and the L-based systems the ^{t}BuA hydrophilic precursor block was deprotected using chemistries that are already well established.[71] This chemistry has been shown not to affect either the structure or function of methyl ester protected, amino acid based acrylamide derivatives.[67] Using trifluoacetic acid (TFA) it is possible to remove the *tert*-butyl group via a nonhydrolytic mechanism that leaves the methyl ester intact and the chirality unaffected (Scheme 4). As a result of the previous work[67] done on a similar system the extent of the deprotection was quantified using primarily ^{1}H NMR spectroscopy (DMSO-d_6). This was carried out by comparing the relative integrals of the signal at δ = 4.19−4.66 (1 acrylamide proton) with the signal at δ = 0.61−2.55 (8 protons from the backbone and isopropyl group of the acrylamide and 12 protons from the backbone and *tert*-butyl group of the ^{t}BuA). Using this technique the deprotection of **7** and **8** were found to have gone to >99% conversion after 24 h. The deprotection was also investigated using infrared spectroscopy and the presence of a broad band centered around 3350 cm^{-1} arising from the stretching of an −OH group was indicative of the free carboxylic acid group. In converting the *tert*-butyl ester to an acid a red shift of ~35 cm^{-1} in the stretching frequency of the carbonyl would be expected, however due to the presence of the methyl ester and the amide groups in the leucine block, the signals overlapped. This mean that qualitative assessment of the red-shifted frequency was difficult although some broadening of the signal at 1659 cm^{-1} accompanied by a distinct change in the peak shape was observed. These observations were noted in both the systems.

*Self-Assembly of P(D-Leu-OMe)-b-P(AA) (**9**) and P(L-Leu-OMe)-b-P(AA) (**10**) To Form Enantiopure Micelles (**11** and **12**) and Racemic Mixed Micelles (**13**).* It is possible to form micelles from amphiphilic diblock copolymers by exploiting the hydrophobic effect and this method has been reported widely in the literature.[72−75] It requires a good solvent for both the hydrophobic and hydrophilic blocks that is miscible with water—both THF and DMF have been used successfully. A solution of the diblock(s) in DMF was made up with an initial polymer concentration in DMF of 1 mg mL^{-1}. The same volume of nanopure water was added dropwise to this rapidly agitated solution via a peristaltic pump at a rate of *ca.* 15 mL min^{-1}. After stirring overnight, the solution was transferred to cellulose membrane bags with a MWCO of 3000 Da and dialyzed exhaustively against nanopure water to remove all of the DMF. The size and shape of the micelles was determined using three different characterization techniques: dynamic light scattering (DLS), transmission electron microscopy (TEM) and atomic force microscopy (AFM). Further information about the chirality of the particles was obtained using circular dichroism (CD) techniques.

It can be seen from the DLS measurements that the two enantiomerically pure systems, **11** and **12**, have similar particle sizes of around 30 nm with reasonably narrow dispersities (0.20 and 0.15 respectively), whereas the mixed system, **13**, is approximately 20 nm larger in size and has a broader PDI (0.44) (Table 5 and Figure 3). Within the pure micelles the polymer chains may be random coils with little or no beneficial interaction occurring between neighboring chains. However, in the mixed system it could be envisaged that a varying degree of interdigitation between the chains upon formation of a stereocomplex prevents the polymer chains from collapsing leading to a larger particle size. Furthermore, because stereocomplexation is not a directed process, the entanglement between chains in the hydrophobic core of each micelle would be different; this could prevent complete alignment between complementary chains occurring resulting in varying degrees of stereocomplexation. The overall result of this could be to increase the PDI of the sample as is observed. This theory is backed up by results obtained when redispersing the lyophilized samples **11** and **13**.

Initial attempts to redissolve **13** in DMF were unsuccessful, and solubilizing the polymer was not possible until after treating the sample with ultrasound, whereas **11** was readily redissolved by stirring the sample in DMF. Redispersion of covalently cross-linked nanoparticles is known to be difficult to achieve and this points toward **13** retaining its particle morphology even after removal of solvent, this could be due to the formation of a heterointeraction in the core. Treatment with ultrasound was sufficient to break the proposed heterocomplex up and allow for redispersion to occur. After dissolving the two samples in DMF, nanopure water was added in the same manner as before to remake the micelles. However this time the solutions were not dialyzed to remove the DMF. Analysis of the two resulting solutions showed that, as expected, the particle diameters were considerably

Scheme 4. Deprotection of the Poly(*tert*-butyl acrylate) Segment of Poly(*tert*-butyl acrylate)-*b*-poly(*N*-acryloyl-D-leucine methyl ester) (7) and Poly(*tert*-butyl acrylate)-*b*-poly(*N*-acryloyl-L-leucine methyl ester) (8) To Afford Amphiphilic Chiral Diblocks, Poly(acrylic acid)-*b*-poly(*N*-acryloyl-D-leucine methyl ester) (9) and Poly(acrylic acid)-*b*-poly(*N*-acryloyl-L-leucine methyl ester) (10)

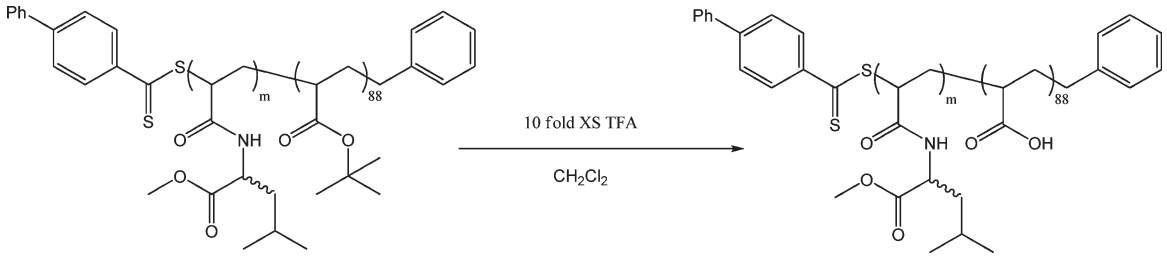

(**7**) and (**9**): $m = 97$
(**8**) and (**10**): $m = 77$

Table 5. Micelle Characterization Data for Poly(acrylic acid)-*b*-poly(*N*-acryloyl-D-leucine methyl ester) (11), Poly(acrylic acid)-*b*-poly(*N*-acryloyl-L-leucine methyl ester) (12), and a 50/50 Blend of Poly(acrylic acid)-*b*-poly(*N*-acryloyl-D-leucine methyl ester) and Poly(acrylic acid)-*b*-poly(*N*-acryloyl-L-leucine methyl ester) (13)

micelle	DLS D_h[a] (nm) (PDI)	TEM D_{av}[b] (nm)
11	32 (0.20)	21 ± 4
12	27 (0.15)	18 ± 5
13	51 (0.44)	31 ± 6

[a] Number-averaged hydrodynamic diameters in aqueous solution by dynamic light scattering. [b] Average diameters were measured by TEM, calculated from the values for 150 particles.

larger (**11** = 289 nm, **13** = 225 nm) than after removal of DMF via dialysis. This is because the chiral cores of the particles are still well solvated by DMF allowing the chains to fill a much bigger volume than when solvent has been removed. What is also evident is that the PDIs of both samples are narrow (**11** = 0.18, **13** = 0.12), in particular the PDI of **13** is considerably narrower (0.12 *cf*. 0.44) than seen in the dialyzed sample. This indicates further that the heterointeraction, and subsequent stabilization, does not occur until the core of the micelle is solvent free: further evidence toward the glassy nature of the core of micelles. This was further confirmed by titration experiments using ^{1}H NMR spectroscopy and IR studies of the homopolymers in solution, in both cases no stereocomplexation was observed.

In other systems, there is quite often a difference seen between light scattering and microscopy data, and the same is true here. While the particle's spherical shape is retained there is a small amount of constriction occurring which is probably due to dehydration of the system upon being subjected to the ultra high vacuum in the TEM (Table 5 and Figure 4). Along with this expected deviation from the fully hydrated particle size being apparent, there is also a small but significant difference between the pure and mixed systems. The mixed micelles are approximately 10 nm larger than the pure micelles and it is again postulated that this is further evidence toward the formation of a strong favorable heterointeraction between the D- and L-leucine moieties within the hydrophobic core of the micelle. If the stereocomplex had formed there would be more order within the core of the micelle which would in turn make it harder for them to collapse when dried on the substrate for TEM analysis.

Attempts to characterize the particles by AFM were inconclusive (see Supporting Information for images). The samples were prepared by drop depositing the solutions onto freshly cleaved mica and, in the first instance, allowed to dry naturally in air. When these samples were imaged the enantiopure samples **11** and **12** appeared to be very polydisperse with

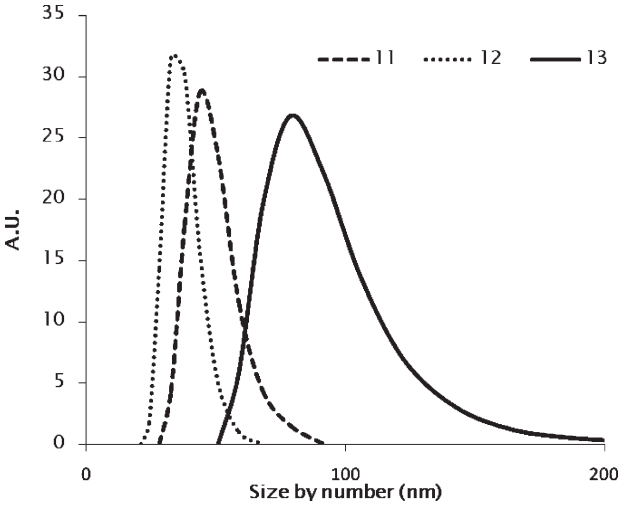

Figure 3. DLS trace of enantiopure poly(acrylic acid)-*b*-poly(*N*-acryloyl-D-leucine methyl ester), **11**, and a 50/50 blend of poly(acrylic acid)-*b*-poly(*N*-acryloyl-D-leucine methyl ester) and poly(acrylic acid)-*b*-poly(*N*-acryloyl-L-leucine methyl ester) racemic micelles, **13**.

particle widths (**11**, $D_{av} = 74 \pm 9$ nm, $H_{av} = 21 \pm 4$ nm; **12**, $D_{av} = 80 \pm 10$ nm, $H_{av} = 12 \pm 3$ nm) that were much larger than would be expected, even after having taken convolution effects from the tip into account. On closer inspection it appeared that the particles were aggregating and falling apart, this goes some way to explaining the discrepancy between the height values of the enantiopure samples. Aggregation was not seen for the racemic system (**13**); in fact, a very monodisperse monolayer of particles was seen on the surface of the mica. However taking into account convolution effects the particle size ($D_{av} = 44 \pm 5$ nm, $H_{av} = 6 \pm 1$ nm) was somewhat smaller than expected. As all of the samples were prepared in the same manner these differences were potentially an artifact of this process. When the TEM samples were prepared the water was completely removed from the sample very rapidly when placed in the ultrahigh vacuum which provided good image clarity. In an attempt to mimic this rapid drying process the AFM samples were incubated at 140 °C for 30 min immediately after drop depositing the solutions onto mica. When the rapidly dried samples were imaged two things were apparent, first the enantiopure micelles (**11** and **12**) had all collapsed and formed a polymer film on the surface of the mica and second that the particles in the racemic system (**13**) were the same size as seen in the slowly dried samples (see ESI). Although not conclusive, these results do provide further evidence toward the presence of a stabilizing interaction within the core of the racemic micelles.

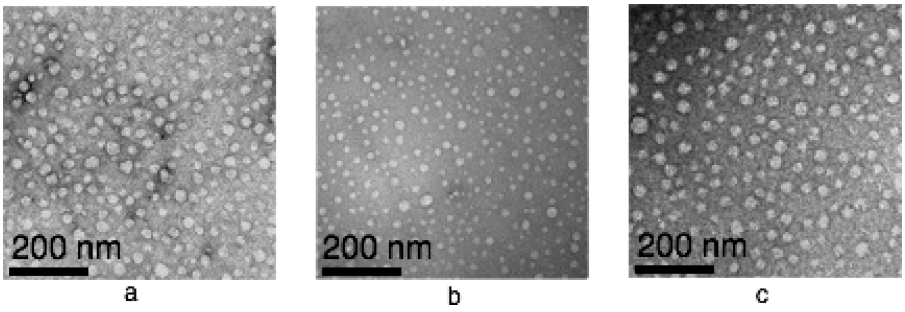

Figure 4. Representative transmission electron microscopy pictures obtained by drop depositing micelle solutions made from (a) poly(acrylic acid)-*b*-poly(*N*-acryloyl-D-leucine methyl ester) (**11**), b) poly(acrylic acid)-*b*-poly(*N*-acryloyl-L-leucine methyl ester) (**12**), and (c) a 50/50 blend of poly(acrylic acid)-*b*-poly(*N*-acryloyl-D-leucine methyl ester) and poly(acrylic acid)-*b*-poly(*N*-acryloyl-L-leucine methyl ester) (**13**), onto copper/carbon grids and staining with 5% uranyl acetate solution.

Using CD spectroscopy (see Supporting Information), it was hoped that evidence of some degree of higher order structure within the micelles would be seen but this was experimentally unachievable; it did, however, provide some information on the retention of chirality of the individual D and L amphiphilic diblocks. In the enantiopure systems there is a distinct signal around 218 nm, in the D system this is a negative response and in the L systems it is a positive response. There is a reversal of sign in these signals (relative to the specific rotation values of the monomers—Table 1); however, other work undertaken on polymers with pendant amino acid derived R groups has shown that polymerization of chiral monomers can cause large changes in specific rotation values (relative to the monomer) so it is possible that the same has occurred in these systems.[67] In the micelles made from the racemic blend of amphiphilic diblock copolymers the only detector response that is seen is baseline noise, this would be expected as there are essentially equimolar amounts of D and L stereocenters present which renders the sample racemic and optically inactive. The presence of these opposing signals in the enantiopure systems, and absence of any signal after blending the copolymers is further evidence toward the facile nature of the polymerization and deprotection chemistries.

Investigations were carried out into the critical micelle concentrations (CMC) of the different populations of micelles however the values obtained were inconclusive. Initial studies were undertaken using pyrene as a fluorescent probe because this technique has been successfully used before to measure the CMC of a similar system.[67] This was not the case using this system, and while the numbers obtained using this technique were in the same range as those reported for a similar system they were not reliable and could not be compared with each other to determine if the stereocomplexed system was more stable.

4. Conclusions

We have shown that in a solid sample of a racemic monomer, *N*-acryloyl-D/L-leucine methyl ester, the functional groups orientate themselves to form a D:L stereocomplex as evidenced by infrared spectroscopy. Subsequently, using RAFT polymerization techniques, we have synthesized with predictable molecular weights, enantiopure homopolymers of *N*-acryloyl-D/L-leucine methyl ester that order themselves in the solid state to preferentially form heterointeractions between the D and L isomers. It is not yet clear if these chiral side chains induce any stereochemistry into the polymer backbone, however this will be explored in future work. Chain extension of ^{t}BuA macroCTAs with these enantiopure monomers yielded enantiopure diblock copolymers with good control over the dispersity of the sample. Additionally we have shown that using facile deprotection chemistries we can produce enantiopure amphiphilic diblock copolymers which undergo self-assembly into micellar structures in mixed solvent systems of dimethylformamide/water. We have characterized these particles using DLS, TEM, AFM, and CD techniques, and we have shown that in the racemic micelles there is a positive interaction that increases the particle stability compared to the enantiopure analogues. While not conclusive, the microscopy and light scattering data also suggests that this interaction is present within—and helps to stabilize—the racemic micelles. It is not yet clear if this difference in stability between the enantiopure and racemic micelles is significant enough that it could be exploited in drug delivery applications. Future work will try to develop monomers with stronger, more energetically favorable stereocomplex motifs that not only exist in the solid state but when dissolved in solvents that promote hydrogen bonding.

Acknowledgment. We thank the Electron Microscopy Facility, Department of Biological Sciences, University of Warwick (Wellcome Trust grant reference: 055663/Z/98/Z) for instrument use and technical support, Michael O'Connell and Prof. Patrick Unwin of The University of Warwick for their assistance in obtaining AFM images and Prof. Alison Rodger for her help in obtaining and analyzing the Circular Dichroism data. The ESPRC, University of Cambridge, Royal Society, and Leverhulme Trust are acknowledged for funding to support this work. The GPC equipment used in this research was obtained, through Birmingham Science City: Innovative Uses for Advanced Materials in the Modern World (West Midlands Centre for Advanced Materials Project 2), with support from Advantage West Midlands (AWM) and part funded by the European Regional Development Fund (ERDF).

Supporting Information Available: Figures showing infrared spectra of monomers and solution IR of polymers, ^{1}H NMR titration experiment data, DMF GPC traces of both hydrophobic diblock copolymers (**7** and **8**), DLS correlograms and correlation functions and AFM images obtained for micelles **11**, **12**, and **13** and text describing these figures more completely. This material is available free of charge via the Internet at http://pubs.acs.org.

References and Notes

(1) Cornelissen, J. J. L. M.; Fischer, M.; Sommerdijk, N. A. J. M.; Nolte, R. J. M. *Science* **1998**, *280*, 1427–1430.
(2) Cornelissen, J. J. L. M.; Rowan, A. E.; Nolte, R. J. M.; Sommerdijk, N. A. J. M. *Chem. Rev.* **2001**, *101*, 4039–4070.
(3) Wooley, K. L. *J. Polym. Sci., Part A: Polym. Chem.* **2000**, *38*, 1397–1407.
(4) Deming, T. J. *Adv. Drug Delivery Rev.* **2002**, *54*, 1145–1155.
(5) Joralemon, M. J.; Smith, N. L.; Holowka, D.; Baird, B.; Wooley, K. L. *Bioconjug. Chem.* **2005**, *16*, 1246–1256.

(6) Sun, X.; Rossin, R.; Turner, J. L.; Becker, M. L.; Joralemon, M., J.; Welch, M. J.; Wooley, K. L. *Biomacromolecules* **2005**, *6*, 2541–2554.
(7) Euliss, L. E.; DuPont, J. A.; Gratton, S.; DeSimone, J. *Chem. Soc. Rev.* **2006**, *35*, 1095–1104.
(8) Matyjaszewski, K.; Nakagawa, Y.; Gaynor, S. G. *Macromol. Rapid Commun.* **1997**, *18*, 1057–1066.
(9) Chen, Y.; Du, J.; Xiong, M.; Guo, H.; Jinnai, H.; Kaneko, T. *Macromolecules* **2007**, *40*, 4389–4392.
(10) Prochazka, K.; Martin, T. J.; Webber, S. E.; Munk, P. *Macromolecules* **1996**, *29*, 6526–6530.
(11) Won, Y.; Davis, H. T.; Bates, F. S. *Science* **1999**, *283*, 960–963.
(12) Discher, D. E.; Ahmed, F. *Ann. Rev. Biomed. Eng.* **2006**, *8*, 323–341.
(13) Discher, D. E.; Eisenberg, A. *Science* **2002**, *297*, 967–973.
(14) Dove, A. P. *Chem. Comm* **2008**, 6446–6470.
(15) Blanazs, A.; Armes, S. P.; Ryan, A. J. *Macromol. Rapid Commun.* **2009**, *30*, 267–277.
(16) O'Reilly, R. K.; Hawker, C. J.; Wooley, K. L. *Chem. Soc. Rev.* **2006**, *35*, 1068–1083.
(17) Pochan, D. J.; Chen, Z.; Cui, H.; Hales, K.; Qi, K.; Wooley, K. L. *Science* **2004**, *306*, 94–97.
(18) Riegel, I. C.; Samios, D.; Petzhold, C. L.; Eisenberg, A. *Polymer* **2003**, *44*, 2117–2128.
(19) Riess, G. *Prog. Polym. Sci.* **2003**, *28*, 1107–1170.
(20) Huang, X.; Du, F.; Cheng, J.; Dong, Y.; Liang, D.; Ji, S.; Lin, S.; Li, Z. *Macromolecules* **2009**, *42*, 783–790.
(21) Magnusson, J. P.; Khan, A.; Pasparakis, G.; Saeed, A. O.; Wang, W.; Alexander, C. *J. Am. Chem. Soc.* **2008**, *130*, 10852–10853.
(22) Zhao, Y.; Bertrand, J.; Tong, X.; Zhao, Y. *Langmuir* **2009**, *25*, 13151–13157.
(23) Sallach, R. E.; Wei, M.; Biswas, N.; Conticello, V. P.; Lecommandoux, S.; Dluhy, R. A.; Chaikof, E. L. *J. Am. Chem. Soc.* **2006**, *128*, 12014–12019.
(24) Kim, B.; Lee, H.; Min, Y.; Poon, Z.; Hammond, P. T. *Chem. Comm* **2009**, 4194–4196.
(25) Kazunori, K.; Glenn, S, K.; Masayuki, Y.; Teruo, O.; Yasuhisa, S. *J. Controlled Release* **1993**, *24*, 119–132.
(26) O'Reilly, R. K.; Joralemon, M. J.; Hawker, C. J.; Wooley, K. L. *New. J. Chem.* **2007**, *31*, 718–724.
(27) Henselwood, F.; Liu, G. *Macromolecules* **1997**, *30*, 488–493.
(28) Wegrzyn, J. K.; Stephan, T.; Lau, R.; Grubbs, R. B. *J. Polym. Sci., Part A: Polym. Chem.* **2005**, *43*, 2977–2984.
(29) Rheingans, O.; Hugenberg, N.; Harris, J. R.; Fischer, K.; Maskos, M. *Macromolecules* **2000**, *33*, 4780–4790.
(30) Thurmond, K. B.; Kowalewski, T.; Wooley, K. L. *J. Am. Chem. Soc.* **1997**, *119*, 6656–6665.
(31) Read, E. S.; Armes, S. P. *Chem. Commun.* **2007**, 3021–3035.
(32) Jiang, X.; Ge, Z.; Xu, J.; Liu, H.; Liu, S. *Biomacromolecules* **2007**, *8*, 3184–3192.
(33) Wang, X.; Liu, K.; Arsenault, A. C.; Rider, D. A.; Ozin, G. A.; Winnik, M. A.; Manners, I. *J. Am. Chem. Soc.* **2007**, *129*, 5630–5639.
(34) Harada, A.; Kataoka, K. *Macromolecules* **2002**, *28*, 5294–5299.
(35) Lavasanifar, A.; Samuel, J.; Kwon, G. S. *Adv. Drug. Del. Rev.* **2002**, *54*, 169–190.
(36) Kakizawa, Y.; Kataoka, K. *Adv. Drug. Del. Rev.* **2002**, *54*, 203–222.
(37) Weaver, J. V. M.; Tang, Y.; Liu, S.; Iddon, P. D.; Grigg, R.; Billingham, N. C.; Armes, S. P.; Hunter, R.; Rannard, S. P. *Angew. Chem., Int. Ed.* **2004**, *43*, 1389–1392.
(38) Chen, L.; Xie, Z.; Hu, J.; Chen, X.; Jing, X. *J. Nano. Res.* **2007**, *9*, 777–785.
(39) Lee, S. C.; Lee, H. J. *Langmuir* **2006**, *23*, 488–495.
(40) Liu, H. Z.; Liu, K.-J. *Macromolecules* **1968**, *1*, 157–162.
(41) Schomaker, E.; Challa, G. *Macromolecules* **1989**, *22*, 3337–3341.
(42) Deuring, H.; Alberda van Ekenstein, G. O. R.; Challa, G.; Mason, J. P.; Hogen-Esch, T. E. *Macromolecules* **1995**, *28*, 1952–1958.
(43) Asai, S.; Kawano, T.; Hirota, S.; Tominaga, Y.; Sumita, M.; Mizumoto, T. *Polymer* **2007**, *48*, 5116–5124.
(44) Tsuji, H. *Macromol. Biosci.* **2005**, *5*, 569–597.
(45) Lee, W.; Iwata, T.; Gardella, J. A. *Langmuir* **2005**, *21*, 11180–11184.
(46) Kim, S. H.; Nederberg, F.; Zhang, L.; Wade, C. G.; Waymouth, R. M.; Hedrick, J. L. *Nano Lett.* **2007**, *8*, 294–301.
(47) Spasova, M.; Mespouille, L.; Coulembier, O.; Paneva, D.; Manolova, N.; Rashkov, I.; Dubois, P. *Biomacromolecules* **2009**, *10*, 1217–1223.
(48) Ikada, Y.; Jamshidi, K.; Tsuji, H.; Hyon, S. H. *Macromolecules* **1987**, *20*, 904–906.
(49) Tsuji, H.; Ikada, Y. *Polymer* **1999**, *40*, 6699–6708.
(50) Kang, N.; Perron, M.-E.; Prud'homme, R. E.; Zhang, Y.; Gaucher, G.; Leroux, J.-C. *Nano Lett.* **2005**, *5*, 315–319.
(51) Kim, S. H.; Tan, J. P. K.; Nederberg, F.; Fukushima, K.; Yang, Y. Y.; Waymouth, R. M.; Hedrick, J. L. *Macromolecules* **2009**, *42*, 25–29.
(52) Rodriguez-Hernandez, J.; Lecommandoux, S. *J. Am. Chem. Soc.* **2005**, *127*, 2026–2027.
(53) Adams, D. J.; Atkins, D.; Cooper, A. I.; Furzeland, S.; Trewin, A.; Young, I. *Biomacromolecules* **2008**, *9*, 2997–3003.
(54) Sanda, F.; Endo, T. *Macromol. Chem. Phys.* **1999**, *200*, 2651–2661.
(55) Murata, H.; Sanda, F.; Endo, T. *Macromolecules* **1996**, *29*, 5535–5538.
(56) Murata, H.; Sanda, F.; Endo, T. *Macromolecules* **1997**, *30*, 2902–2906.
(57) Sanda, F.; Abe, T.; Endo, T. *J. Polym. Sci., Part A: Polym. Chem.* **1996**, *34*, 1969–1975.
(58) Mori, H.; Iwaya, H.; Nagai, A.; Endo, T. *Chem. Commun.* **2005**, 4872–4874.
(59) Mori, H.; Matsuyama, M.; Sutoh, K.; Endo, T. *Macromolecules* **2006**, *39*, 4351–4360.
(60) Sanda, F.; Nakamura, M.; Endo, T. *Macromolecules* **1996**, *29*, 8064–8068.
(61) Lokitz, B. S.; Stempka, J. E.; York, A. W.; Li, Y.; Goel, H. K.; Bishop, G. R.; McCormick, C. L. *Aust. J. Chem.* **2006**, *59*, 749–754.
(62) Chou, P. Y.; Wells, M.; Fasman, G. D. *Biochem.* **1972**, *11*, 3028–3043.
(63) Chou, P. Y.; Fasman, G. D. *J. Mol. Biol.* **1973**, *74*, 263–281.
(64) Sanda, F.; Nakamura, M.; Endo, T. *J. Polym. Sci., Part A: Polym. Chem.* **1998**, *36*, 2681–2690.
(65) Gao, H.; Isobe, Y.; Onimura, K.; Oishi, T. *J. Polym. Sci., Part A: Polym. Chem.* **2007**, *45*, 3722–3738.
(66) Sanda, F.; Abe, T.; Endo, T. *J. Polym. Sci., Part A: Polym. Chem.* **1997**, *35*, 2619–2629.
(67) Skey, J.; O'Reilly, R. K. *J. Polym. Sci., Part A: Polym. Chem.* **2008**, *46*, 3690–3702.
(68) Marin, R.; de Ilarduya, A. M.; Romero, P.; Sarasua, J. R.; Meaurio, E.; Zuza, E.; Munoz-Guerra, S. *Macromolecules* **2008**, *41*, 3734–3738.
(69) Barner-Kowollik, C.; Buback, M.; Charleux, B.; Coote, M. L.; Drache, M.; Fukuda, T.; Goto, A.; Klumperman, B.; Lowe, A. B.; McLeary, J. B.; Moad, G.; Monteiro, M. J.; Sanderson, R. D.; Tonge, M. P.; Vana, P. *J. Polym. Sci., Part A: Polym. Chem.* **2006**, *44*, 5809–5831.
(70) Vana, P. *Macromol. Symp.* **2007**, *248*, 71–81.
(71) O'Reilly, R. K.; Joralemon, M. J.; Wooley, K. L.; Hawker, C. J. *Chem. Mater.* **2005**, *17*, 5976–5988.
(72) Buetuen, V.; Billingham, N. C.; Armes, S. P. *J. Am. Chem. Soc.* **1998**, *120*, 12135–12136.
(73) Kataoka, K.; Harada, A.; Nagasaki, Y. *Adv. Drug Delivery Rev.* **2001**, *47*, 113–131.
(74) Lokitz, B. S.; Convertine, A. J.; Ezell, R. G.; Heidenreich, A.; Li, Y.; McCormick, C. L. *Macromolecules* **2006**, *39*, 8594–8602.
(75) Ge, Z.; Xie, D.; Chen, D.; Jiang, X.; Zhang, Y.; Liu, H.; Liu, S. *Macromolecules* **2007**, *40*, 3538–3546.